Response of Initially Bent and Imperfect Piles to Vertical Loads

by

K. Kurma Rao*

H. Krishna Murthi*

Introduction

IT is difficult to drive a pile so that it is absolutely straight. In most foundation projects where driven pipe or cast-in-place piling is used or where the piling is installed in long lengths, it is commonly found that some of the piles get bent during installation. There were instances in which two piles formed a conjuctive (U) so that one rose while the other was driven down and vice versa (Johnson, 1968). According to Cummings (1956), piles are sometimes distorted into long pitch helical curves, sometimes into long sweeping bends and occasionally into sharp bends, called dog-legs. Hanna (1968) investigated long H-piles and found that very small bending radii of about 60 m occurred, inducing stresses in the pile section well exceeding the normally accepted values. Hanna (1968) has demonstrated, with the help of inclinometer measurements that initially bent piles do bend further under vertical loads. Consequently there will be additional lateral deflections. Fellenius (1972) dealt with the bending of slender precast concrete piles with double curvature. Kim et al (1973) reported that the vertical H-piles installed in groups have deflected about the weak axis of the pile section during driving. Response of such piles to vertical loads is presented in this investigation.

Bent and Imperfect Piles

Piles are expected and designed to be straight. No structure can be made without some initial imperfection in shape. The centre line of even the best pile would show before driving initial deviations from the perfect straight line. Such a pile is considered to be imperfect. When the pile is smoothly and uniformly curved without any sharp kinds, during driving, it is called a bent pile. The bending can be in one or more planes.

Figure 1 shows the schemtaic diagram for a pile under the action of an axial force. The soil modulus is assumed to be constant with depth for cohesive soils as represented in Figure 2. The pile is idealised as a beam and the soil as a Winkler medium, characterised by the modulus of the subgrade reaction. Figure 3 shows the pinned-pinned and Fixed-Fixed imperfect piles. Pinned-pinned and Fixed-Pinned Bent Piles are also shown in the same figure.

---

* Assistant Professors in Civil Engineering, College of Engineering, Kakinada, J.N.T. University, Andra Pradesh, India.

This paper was received in April, 1980 and is open for discussion till the end of January 1982.

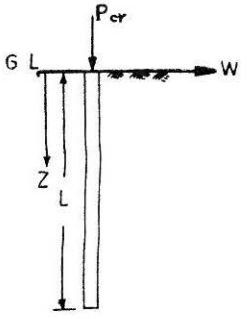

FIGURE 1 Pile under the action of an axial load

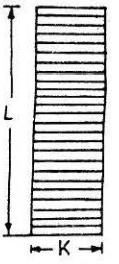

FIGURE 2 Variation of soil modulus with depth

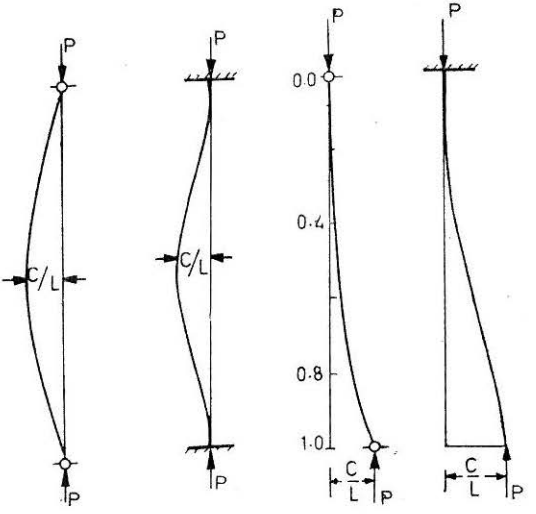

(*a*) Pinned-Pinned (*b*) Fixed-Fixed (*c*) Pinned-Pinned (*d*) Fixed-Pinned

FIGURE 3 Pile boundary conditions

Imperfect Pile with Pinned-Pinned End Conditions

Very long piles may develop large deviations near the centre of their length and they may be approximated by a half sine curve as shown in Figure 3. The initial shape satisfying the boundary conditions may be represented by

$$W_1 = \frac{C}{L} \operatorname{Sin} \pi Z \qquad \ldots (1)$$

where $\frac{C}{L}$ is the non-dimensionalized offset of the pile at the centre of its length; W_1 is the initial deflection of the pile from the vertical axis and Z is the non-dimensionalized depth from ground. The function W_1 need satisfy both geometric and natural boundary conditions of the problem. The geometric boundary conditions refer to deflection and slope and natural boundary conditions refer to bending moment and shear at the

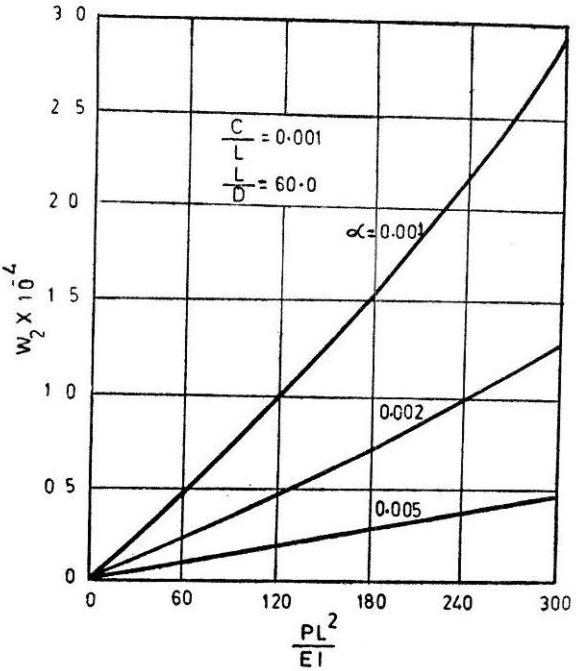

FIGURE 4 Relationship between load and additional deflection for different soil modulii for pinned-pinned imperfect pile

boundaries. Equation (1) satisfies the explicit geometric conditions

$$(W_1)_{z=0};\ (W_1)_{z=1\cdot0} = 0 \qquad \ldots (2a)$$

as well as implicit geometric boundary conditions,

$$\left(\frac{dW_1}{dZ}\right)_{z=0} \neq 0 \text{ and } \left(\frac{dW_1}{dZ}\right)_{z=1} \neq 0. \qquad \ldots (2b)$$

The explicit equilibrium boundary conditions

$$\left(\frac{d^2W_1}{dZ^2}\right)_{z=0} = 0;\ \left(\frac{d^2W_1}{dZ^2}\right)_{z=1} = 0 \qquad \ldots (2c)$$

as well as implicit equilibrium boundary conditions

$$\left(\frac{d^3W_1}{dZ^3}\right)_{z=0} \neq 0;\ \left(\frac{d^3W_1}{dZ^3}\right)_{z=1} \neq 0 \qquad \ldots (2d)$$

are satisfied.

The governing differential equation representing the force system on the pile for the constant moment of inertia I and load P was given by Marcus and was reported by Johnson (1968). The non-dimensionalized form of the same is given by Kurma Rao (1975) as below

$$\frac{d^4W_2}{dZ^4} + \alpha_1 \frac{d^2W_1}{dZ^2} + \alpha_2 W_2 = -\alpha_1 \frac{d^2W_1}{dZ^2} \qquad \ldots (3)$$

where $\alpha_1 = \frac{PL^2}{EI}$; $\alpha_2 = \frac{kD}{EI}$. L^4; W_2 = additional non-dimensionalized deflection under the load P; k = soil modulus of the pile and D = diameter of the pile.

Substituting Equation 1 in Equation 3, the governing differential equation for pin-pin end conditions of an imperfect pile may be written as

$$\frac{d^4W_2}{dZ^4} + \alpha_1 \frac{d^2W_2}{dZ^2} + \alpha_2 W_2 = \alpha_1 \pi^2 \frac{C}{L}. \text{ Sin } \pi Z \qquad \ldots (4)$$

Let the particular solution of Equation 4 be

$$W_2' = A \text{ Sin } \pi Z \qquad \ldots (5)$$

where the constant, A, can be obtained as

$$A = \frac{\pi^2 \alpha_1 C}{L(\pi^4 - \alpha_1 \pi^2 + \alpha_2)} \qquad \ldots (6)$$

The solution for homogeneous part of Equation (4) is

$$W_2'' = C_1 \text{ Sin } (m_1 Z). \cos h\ (m_2 Z) + C_2 \cos (m_1 Z). \sin h\ (m_2 Z) +$$

$$D_1 \sin (m_1 Z). \sin h\ (m_2 Z) + D_2 \cos (m_1 Z). \cos h\ (m_2 Z) \qquad \ldots (7)$$

where C_1, C_2, D_1 and D_2 are constants to be determined by boundary conditions and

$$m_1^2 = \sqrt{\frac{\alpha_2}{4}} + \frac{\alpha_1}{4} \text{ and } m_2^2 = \sqrt{\frac{\alpha_2}{4}} - \frac{\alpha_1}{4}$$

Substituting the following four boundary conditions, the constants C_1, C_2, D_1 and D_2 can be evaluated.

when $Z = 0$, $W_2 = W_2' + W_2'' = 0$ and $\frac{d^2W_2}{dZ^2} = 0$ ... (7*a*)

$$Z = 1,\ W_2 = W_2' + W_2'' = 0 \text{ and } \frac{d^2W_2}{dZ^2} = 0 \qquad \ldots (7b)$$

Solving Equations 7*a* and 7*b*, the constants C_1, C_2, D_1 and D_2 are found to be zero and therefore the homogeneous part of the solution becomes zero in case of pinned pinned end conditions.

Imperfect Pile with Fixed-Fixed End Conditions

The initial shape can be represented as

$$W_1 = 0.5 \frac{C}{L} (1 - \cos 2\pi Z) \qquad \ldots (8)$$

The governing differential equation for fixed-fixed end conditions of the imperfect pile may be obtained by substituting Equation 8 in Equation 3 and let the particular solution be

$$W_2' = A \cos 2\pi Z \qquad \ldots (9)$$

where $$A = \frac{2\pi^2 \alpha_1 C/L}{(16\pi^4 - 4\pi^2 \alpha_1 + \alpha_2)}$$

Substituting the appropriate boundary conditions, the constants C_1, C_2, D_1 and D_2 pertaining to homogeneous part can be obtained and are presented in matrix form as

$$\begin{bmatrix} 0 & 0 & 0 & 1 \\ m_1 & m_2 & 0 & 0 \\ R & S & T & U \\ I & J & K & L \end{bmatrix} \begin{bmatrix} C_1 \\ C_2 \\ D_1 \\ D_2 \end{bmatrix} = \begin{bmatrix} -A \\ 0 \\ -A \\ 0 \end{bmatrix} \quad \ldots (10)$$

where $$I = m_1 U + m_2 . T; \quad J = m_2 U - m_1 T$$

$$K = m_2 R + m_1 . S; \quad L = m_2 S - m_1 R$$

$$R = \sin m_1 . \cosh m_2; \quad S = \cos m_1 . \sinh m_2$$

$$T = \sin m_1 . \sinh m_2; \quad U = \cos m_1 . \cosh m_2$$

Bent Pile with Pinned-Pinned End Conditions

The initial shape for pinned-pinned boundary conditions in non-dimensional form may be represented as

$$W_1 = \frac{0.5\ C}{L\ (KL - \sin KL)} (2KLZ + KLZ \cos KLZ - 3 \sin KLZ) \quad \ldots (11)$$

where KL is the root of the transcendental equation $\tan KL = KL$.

One of the roots is $4.494 \frac{C}{L}$ is the offset of the pile tip from the vertical axis.

The governing differential equation for pinned-pinned end conditions of bent piles may be obtained by substituting Equation 11 in Equation 3 and the particular solution may be presented as

$$W_2' = A \sin (KL.Z) - B.KL.Z \cos (KL.Z) \quad \ldots (12)$$

where $$B = \frac{D_1}{F_1}; \quad D_1 = \frac{(KL)^2 . \alpha_1}{2\ (KL - \sin KL)} \frac{C}{L}$$

$$F_1 = (KL)^4 - \alpha_1 (KL)^2 + \alpha_2 \quad \ldots (12a)$$

$$A = \frac{B[4(KL)^4 - 2\alpha_1 (KL)^2] - D_1}{F_1}$$

The constants C_1, C_2 and D_1 and D_2 that are related to the homogeneous part can be obtained by following boundary conditions.

$$\text{For } Z = 0 \text{ and } Z = 1 \quad W_2 = 0 \text{ and } \frac{d^2 W_2}{dZ^2} = 0 \quad \ldots (12b)$$

Fixed-Pinned Bent Pile

In dimensionless form, the initial shape for fixed-pinned boundary conditions, may be represented by

$$W_1 = \frac{C}{L}\left(1-\cos\frac{\pi Z}{2}\right) \qquad \ldots (13)$$

The solution to Equations 3 and 13 can be obtained similar to the previous cases substituting the following four boundary conditions.

$$\text{For } Z = 0 \; W_2 = W_2' + W_2'' = 0 \text{ and } \frac{dW_2}{dZ} = 0$$

$$Z = 1.0, \; W_2 = W_2' + W_2'' = 0 \text{ and } \frac{d^2W_2}{dZ^2} = 0 \qquad \ldots (14)$$

The total additional deflection under load P is

$$W_2 = W_2' + W_2'' \qquad \ldots (15)$$

Radius of Curvature

The radius of curvature of the pile can be obtained from the relationship

$$R = \frac{L}{\frac{d^2W}{dZ^2}} \qquad \ldots (16)$$

where $W = W_1 + W_2$. Equation 16 may also be written as

$$\frac{R}{D} = \frac{L/D}{\frac{d^2W}{dZ^2}} \qquad \ldots (17)$$

Load Carrying Capacity of Bent Pile

The load carrying capacity of straight R.C.C. pile when loaded axially is given by (Johnson, 1968),

$$P_S = 0.85 \; R \; A_g \; (0.25 \, f_c' + f_s \, p_g) \qquad \ldots (18)$$

where P_s = allowable axial load on pile; R = reduction factor for length, A_g = gross area of column, f_c' = compressive strength of concrete, f_s = allowable stress in column reinforcement, P_g = ratio of area of vertical reinforcement to gross area of columm. R is taken as unity in this investigation.

$$\text{The allowable stress } S = \frac{P_S}{A_g} \qquad \ldots (19)$$

In case of bent pile, three types of stresses, namely, the residual stress S_1, the bending stress S_2, under the load P_b on bent pile and the axial stress S_3 are acting and they are cumulative. The load on the bent

pile P_b is obtained by satisfying the condition,

$$\frac{S_1+S_2+S_3}{S} \leqslant 1.0 \qquad \ldots(20)$$

Equation. 20 is solved for P_b using iterative procedure until the ratio is within an error of $\pm$ 0.0001.

Results and Discussion

The maximum values of the additional deflection, W_2, that occur along the depth of a round pile under different loads, P are evaluated from Equations 5 and 7 and plotted in Figure 4 for a pinned-pinned imperfect pile for $\frac{C}{L} = 0.001$; $\frac{L}{D} = 60$ for different values of soil modulii, $\alpha = \frac{64\,kD}{\pi E_c}$. It is observed from the figure that these deflections increase almost linearly with load. For lesser values of soil modulus ($\alpha = 0.001$), it is observed that the relationship is slightly non-linear.

From the figure it may also be concluded that as the value of soil modulus increases, the additional deflection, W_2, decreases, the loading being the same in both the cases. Figure 5 shows similar relationship for

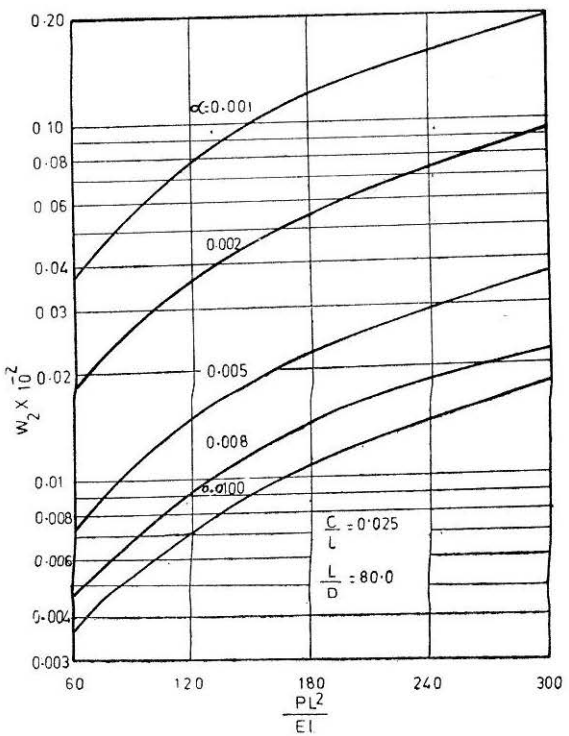

FIGURE 5 Relationship between load and additional deflection for different soil modulii for pinned-pinned imperfect pile

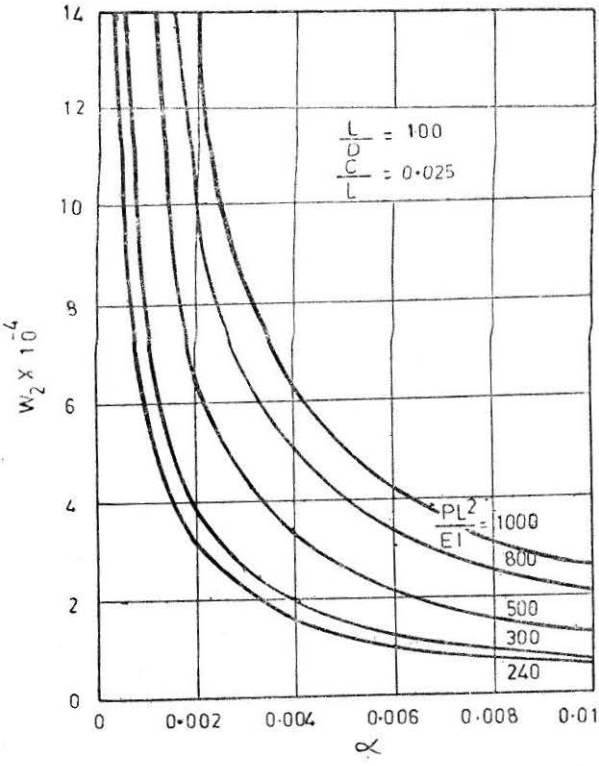

FIGURE 6 Relationship between soil modulus and additional deflection for different vertical loads for pinned-pinned imperfect pile

$\frac{C}{L} = 0.025$ and $\frac{L}{D} = 80$ for various soil modulii, $\alpha = 0.001, 0.002, 0.005, 0.008$ and 0.01, the only difference being that W_2 is plotted on a log scale to accommodate the wide variation of W_2 with α and $\frac{PL^2}{EI}$. The practical range of values of α_1 and α_2 are 50 to 300 and 250 to 1,00,000 respectively. Figure 6 shows the relationship between α and W_2 for various loading conditions. It is observed that the variation of W_2 with soil modulus α for different loads decreases with increase of the soil modulus. Figures 7 and 8 represent the relationsip between the non-dimensionalized radius of curvature $\frac{R}{D}$ and the additional deflection W_2 for fixed-fixed imperfect pile and pinned-pinned bent pile, respectively The response is found to be linear in both the cases and as $\frac{R}{D}$ increases, the additional lateral deflection is found to decrease. In the same figures, relationship between $\frac{R}{D}$ and percentage $\frac{P_b}{P_s}$ is also drawn. P_b represents the load carrying capacity of bent or imperfect

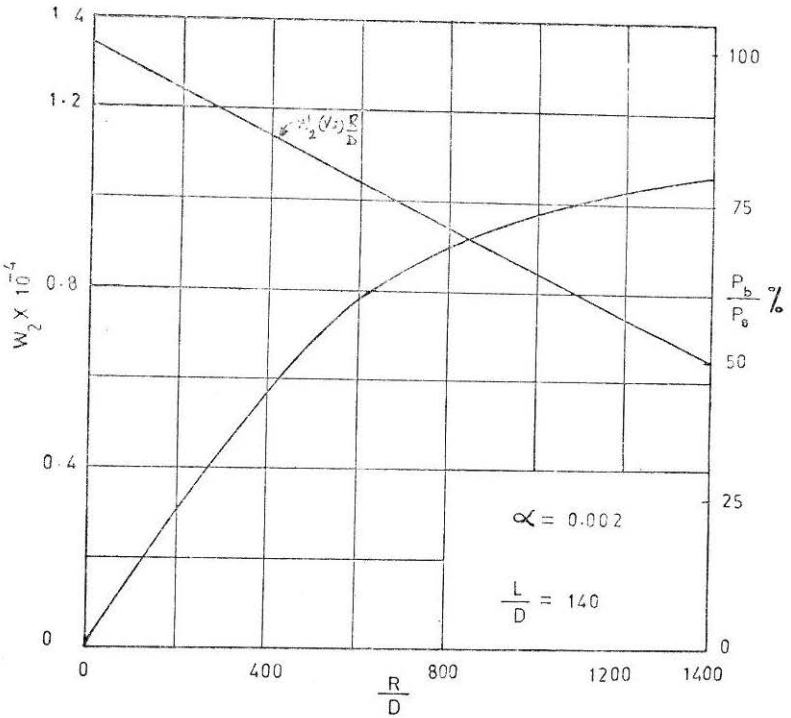

FIGURE 7 Additional deflection and load carrying capacity of fixed-fixed imperfect pile with respect to radius of curvature

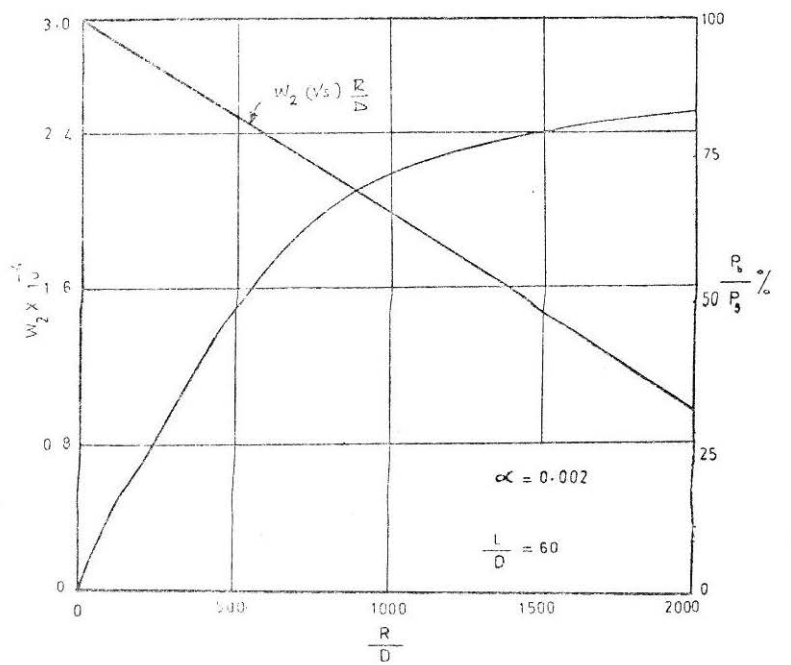

FIGURE 8 Additional deflection and load carrying capacity of pinned-pinned bent pile with respect to radius of curvature

pile as the case may be and P_S relates to the load carrying capacity of a straight pile. The relationship in both the cases is non-linear and unique irrespective of the shape and end-conditions.

Figure 9 shows a relationship between $\frac{PL^2}{EI}$ and W_2 for fixed-pinned bent pile for three different soil modulii. The relationship is linear as is the case with the earlier types. This type of linear behaviour may be attributed to the assumption that the soil modulus is invariant with depth while formulating the governing differential Equation 3 for pile-soil system (Madhav et al, 1975). From Figure 9 it may also be concluded that for a given load, the additional deflection W_2 decreases as the value of soil modulus increases. Figure 10 represents a linear relationship between

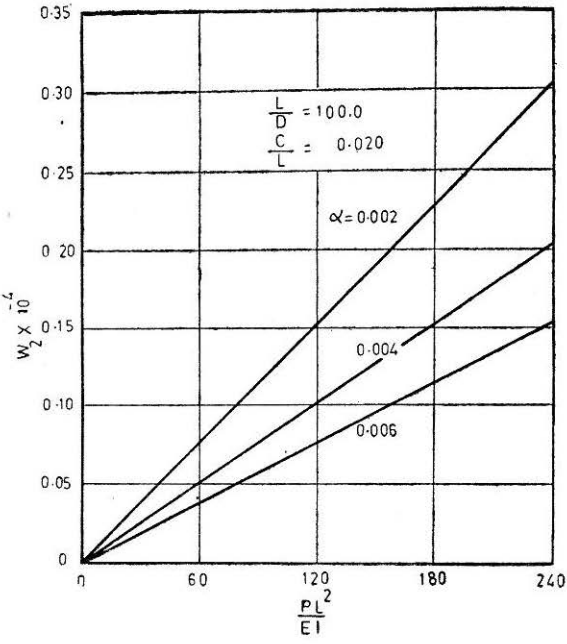

FIGURE 9 Relationship between load and additional deflection for different soil modulii for fixed-pinned bent pile

$\frac{R}{D}$ and W_2 for three soil modulii. At approximately $\frac{R}{D} = 1275$, these lines merge on the horizontal axis. In case of a Fixedhinged bent pile, for $\frac{R}{D}$ ratios equal to 1275 or more, there will not be any lateral additional deflection when loaded.

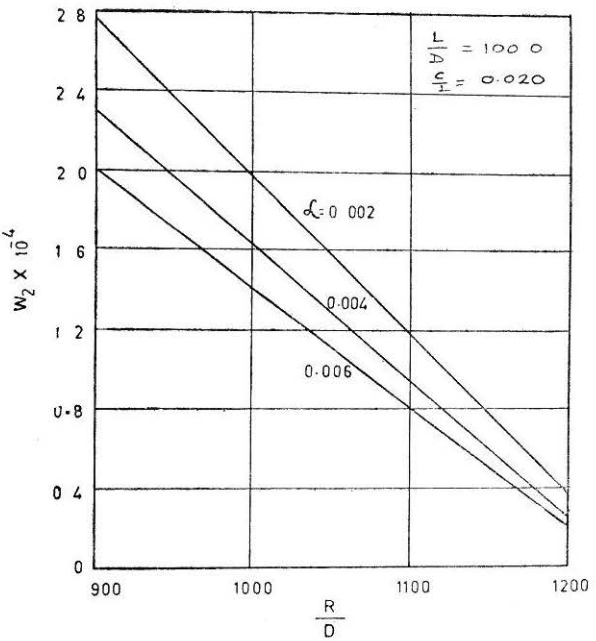

FIGURE 10 Relationship between radius of curvature and additional deflection of pile for different soil modulii for fixed-pinned bent pile

Conclusions

The response of imperfect and bent piles to vertical loads is studied in this investigation. Initially bent and imperfect piles do bend further under load and the maximum additional deflection are found to be proportional to load. It is also observed in this investigation that the additional deflection decreases with increase of soil modulus, other things being same.

References

CUMMINGS, A.E., (1956). "Discussion on Parsons and Wilson Paper, *Transactions ASCE,* Vol. 121, pp. 717-720.

FELLENIUS, B.H., (1972). "Bending of Piles Determined by Inclinometer Measurements". *Canadian Geotechnical Journal.* Vol. 9, pp. 25-31.

HANNA, T.H., (1968). "The Bending of Long H-Section Piles," *Canadian Geotechnical Journal,* Vol. 5(3), pp. 150-172.

JAI B. KIM, ROBERT J.B., CARL H. KINDIG, JOHN L.G., and SINGH L.P., (1973). "Lateral Load Tests on Fullscale Pile Groups in Cohesive Soils," *Ph. D. Research Project,* Bucknell University, Lewisburg, Pennsylvenia.

JOHNSON, S.M., and KAVANAGH, T.C., (1968). "*The Design of Foundation For Buildings,* McGraw-Hill Book Company, New York.

MADHAV, M.R. and KURMA RAO, K., (1975). "Analysis of Initially Bent Piles," *Symposium on Recent Developments in the Analysis of soil Behaviour and their Application to Geotechnical Structures,* The University of New South Wales, pp. 145-155.

KURMA RAO, K (1975). "Analysis of Initially Bent and Imperfect Piles"— *A thesis submitted in partial fulfilment of the requirements for the Degree of Doctor of Philosophy, Indian Institute of Technology, Kanpur (India).*

Failure Mode of Soils During Static and Dynamic Penetration

by

Umesh Dayal*

Introduction

Well established bearing capacity formulae are available for estimation of foundation load for static condition. Most of these formulae are derived by assuming a failure pattern based on laboratory studies and field performance. The demands of foundation that are properly designed for dynamic load have increased the need for further research effort. The proper design of foundation for dynamic load requires a clear understanding of various factors such as the strain rate effect, inertial effect, and modes of failure. The first two factors are broadly discussed by Whitman (1970) and for a particular case of low velocity penetration by Dayal and Allen (1975). The scope of the present paper is limited to third factor, i.e. modes of failure during dynamic loading.

In order to study the difference, if any, in failure pattern during dynamic loading, constant velocity penetration tests were performed on a two dimensional target. The experiments provided a means of viewing sub-surface soil movement associated with penetration of the penetrator. The tests were performed at velocities ranging from 0.0044 fps (0.13 cm/s) to 2.662 fps (81.14 cm/s) onto the soil target varied from gravelly sand through to clay of various strength and moisture content.

The Experimental Procedure

The experiments consisted of driving a penetrator in to a prepared soil target at various speeds. The penetrator was coupled to a hydraulic actuator which in turn was connected to a structural laboratory's 'Material Testing System' (M.T.S.) which provided the required velocity and controlled penetration. The velocity and penetration depth for any particular test could be adjusted from M.T.S. speed and stroke console. The maximum velocity of 2.66 fps (81.1 cm/s) and a stroke of 2 ft (61 cm) could be obtained from this system.

The target tank used for this test was 12 in. (30.5 cm) wide by 24 in. (61 cm) high and 1.5 in. (3.8 cm) thick so that either a half-sectional or a complete - rod penetrator of 1.4 in. (35.6 mm) diameter could enter with mininum friction on its front or back. The front face of the target tank was of 3/4 in. (19 mm) thick plexiglas to permit observations of the movement of the target material during penetration.

To facilitate the visual observations of the movement of the soil, a reference grid was required. Following the required compaction, the

*Assistant Professor, Department of Civil Engineering, Indian Institute of Technology, Kanpur-208016, India.

This paper was received in August, 1980 and is open for discussion till the end of January, 1982.